

Estimation and Monitoring of Bare Soil/Vegetation Ratio With SPOT VEGETATION and HRVIR

Grégoire Mercier, *Member, IEEE*, Laurence Hubert-Moy, Thomas Houet, and Pascal Gouéry

Abstract—Covering soils with vegetation during the fallow and planting seasons is one of the main ways to reduce water pollution, by restricting pollutant fluxes to aquatic systems. The bare soil/vegetation ratio monitoring can be carried out daily with a coarse spatial resolution using SPOT VEGETATION (1 km). Nevertheless, land-cover changes detected at a regional scale with this ratio may be due to winter vegetation cover changes as well as the influence of climatic events. Therefore, observed changes have to be validated from a local-scale analysis with higher spatial resolution data. The aim of this study is to develop a technique that allows high or low variations detected at a regional scale to be assessed from SPOT VEGETATION images with data acquired at a higher scale, SPOT High Resolution Visible and Infrared images in our case. In this study, the link between the images from the two sensors is achieved from the design of an artificial neural network method based on a Kohonen self-organizing map. The originality of this method lies in the use of external knowledge from ground observations and the use of temporal behavior to solve such a change of scale. Results of testing this method by using a potential change map based on the last few years' land-cover observations have shown a good correspondence between the observed and predicted bare soil/vegetation balance with regards to the spatial resolution difference between the two sensors.

Index Terms—Agriculture, neural networks, remote sensing, unmixing.

I. INTRODUCTION

MONITORING land cover during the fallow and planting seasons is an important issue for water pollution reduction in intensive agricultural areas. The removal of surface vegetation leaves soils exposed to intense and damaging rainfall. Vegetation cover has several impacts on water pollution management: it protects soils from raindrop impact and splash, it tends to slow down surface runoff, it allows excess surface water to infiltrate, and it consumes some of the excessive nitrogen in soils. In

Manuscript received March 29, 2004; revised September 16, 2004. This work was supported by the French National Remote Sensing Program (PNTS).

G. Mercier is with the Groupe des Ecoles de Telecommunications Ecole Nationale Supérieure des Télécommunications (GET-ENST Bretagne), Information Technology Department, Centre National de la Recherche Scientifique (CNRS FRE 2658), Traitement Algorithmique et Matériel de la Communication, de l'Information et de la Connaissance (TAMCIC), TIME Team, 29238 Brest Cedex, France (e-mail: gregoire.mercier@enst-bretagne.fr).

L. Hubert-Moy and P. Gouéry are with the Climat et Occupation du Sol par Télédétection (COSTEL), UMR 6554, CNRS-LETG, Université Rennes 2, 35043 Rennes Cedex, France.

T. Houet is with the Groupe des Ecoles de Telecommunications Ecole Nationale Supérieure des Télécommunications (GET-ENST Bretagne), Information Technology Department, Centre National de la Recherche Scientifique (CNRS FRE 2658), Traitement Algorithmique et Matériel de la Communication, de l'Information et de la Connaissance (TAMCIC), TIME Team, 29238 Brest Cedex, France and also with the Climat et Occupation du Sol par Télédétection, UMR 6554, CNRS-LETG, Université Rennes 2, 35043 Rennes Cedex, France.

Digital Object Identifier 10.1109/TGRS.2004.841628

TABLE I
CHARACTERISTICS OF THE SENSORS

	HRVIR High Resolution in Visible and Infra Red	VEGETATION
Host	SPOT-4	SPOT-4 & 5
Spatial Resolution	20m	1km
Swath width	60km	2200km
Spectral Resolution	B1: 0.5–0.59 μm B2: (R) 0.61–0.68 μm B3: (NIR) 0.78–0.89 μm B4: (MIR) 1.58–1.75 μm	B0: 0.43–0.47 μm

Only (R,NIR,MIR) are considered in the fusion process since bands of B0 and B1 differ in spectral location.

fact, vegetation cover reduces pollutant fluxes to aquatic systems [1]. Thus, the bare soil/vegetation ratio is a relevant indicator of farming practices with regards to environmental pollution. But when estimated from large-scale remotely sensed data, this ratio may reflect land-cover variations as well as climatic factor influences [2]. Then, a local analysis has to be performed to validate the large-scale estimation of the ratio. In addition, land use decisions occur both at large and local spatial scales, which correspond to the levels of intervention of some institutions through water quality management programs. Also, all farmers and land managers in the Brittany region in western France are encouraged to cover their soils in winter, which corresponds to the rainy and fallow season in this area. Nevertheless, farmers choose to follow these new environmentally driven incentives or not, some of them still leaving soils without any cover crops.

Remote sensors provide different ways of monitoring vegetation cover during the fallow periods, depending on their spatial resolution. SPOT VEGETATION can offer a daily estimation of the bare soil/vegetation ratio at a large scale—1 km a pixel. SPOT High Resolution Visible and Infrared (HRVIR) can give an estimation of the ratio, but at a finer scale—20 m a pixel—for smaller regions and only once or twice per winter in Brittany (see Table I for a detailed description of these two sensors). Thus, the conjunction of fine- and coarse-resolution data presents several advantages: to obtain a finer resolution of an observation acquired at a coarse scale and then understand changes observed at a larger scale; to guarantee a regular observation and avoid missing data at key periods. When no data are available, it is necessary to simulate a higher resolution observation from the coarse acquisition, taking into consideration previous data to integrate the temporal behavior of land-cover changes. The goal of this study is to make an estimation of the finer scale observation that would have to be acquired, given a large-scale acquisition. This local estimation is necessary to explain abrupt or trend variations of winter land cover, while having only the SPOT VEGETATION observation.

II. MULTISOURCE MULTIREOLUTION IMAGE FUSION

Several algorithms have been proposed in the literature for processing images acquired from sensors at different scales. Most of them prove to have limitations when applied to SPOT HRVIR and SPOT VEGETATION images with an interscale factor of 50. Moreover, our purpose is not to yield a sole product from two observations at different scales but to perform an estimation at a fine scale of ground state from a coarser observation (coming from VEGETATION), from ground observations and from older fine-scale observations (coming from HRVIR). Multiresolution image fusion may be divided into several groups:

Multiscale analysis is a natural way to represent data at different scales and to mix or replace part of the information from the coarse observation. This process can be implemented with a wavelet transform [3]–[5], a Laplacian pyramid [6], or similar strategies of decomposition [7]. This point of view has proved to be powerful to fuse data with a small difference in resolution [such as SPOT HRVIR and Landsat Thematic Mapper (TM)], but it is not appropriate to deal with a large gap of resolution between the sources.

Statistical models are of interest, since they can deal with *a priori* knowledge or strong modeling. They can be applied to a multiresolution [8], [9] or multiscale [10], [11] representation of the data. Evidential models may also be used to fuse heterogeneous data from different scales [12] with a better flexibility than Bayesian techniques.

Fusion methods are based on spectral and spatial information to improve the characterization of objects. Some of them are based on a radiometric combination (panchromatic and multispectral). Cliche's, Brovey's, intensity–hue–saturation, or principal component analysis methods are among the most representative [13]–[15]. Nevertheless, it is considered that these approaches are relevant for visual interpretation, since spatial characterization is integrated into the spectral point of view and radiometric distortion may be significant. Other fusion methods may be well-founded, based on interpolation [16], classification [17], [18] or on structural representation of the data [19].

Unmixing methods may be thought of as disintegration where a coarse observation has to be characterized using finer elementary components. Images of fine resolution can be used to find the spectral signatures of those endmembers, while the samples of the coarse-resolution image have to be decomposed into membership values of the endmembers. These methods may fit the interscale ratio of SPOT VEGETATION and HRVIR (see [20] for SPOT HRVIR and National Oceanic and Atmospheric Administration (NOAA) Advanced Very High Resolution Radiometer (AVHRR) fusion; see [21] for Landsat TM and NOAA AVHRR fusion or [22] for SPOT HRVIR and SPOT VEGETATION fusion). Nevertheless, unmixing techniques are mostly dedicated to superspectral or hyperspectral data. In addition, it is not possible to add the spatial location of the endmembers and then to analyze at a finer scale a change detected at a coarse scale.

Neural methods are of interest for this topic. One of the advantages of this approach is the integration of temporal knowledge into a spatially oriented fusion process. ARTMAP models (based on adaptive resonance theory) have been applied for unmixing purposes [23], cellular neural networks for multiscale

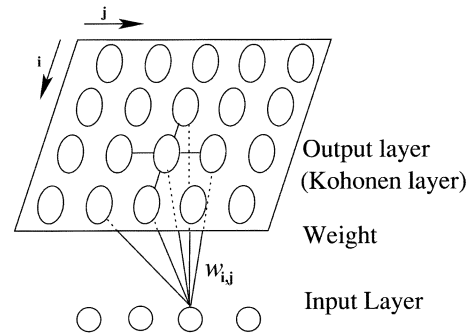


Fig. 1. Kohonen map with 4×5 neurons.

fusion [24] and multilayer perceptron (MLP) for multitemporal multisensor image classification [25]. A superresolution technique has been developed through a Hopfield network by Tatem [26]. As it stands, this last approach does not fit the interscale ratio of SPOT VEGETATION and SPOT HRVIR.

It is proposed, in this study, to achieve spectral unmixing of SPOT VEGETATION observations with the spatial location of endmembers by integrating temporal knowledge of previous SPOT HRVIR observations within a Kohonen self-organizing map (SOM).

III. KOHONEN MAP

A. Network Design

The SOM is a neural network algorithm proposed by Kohonen [27] that forms a two-dimensional presentation of multidimensional data. Kohonen maps have been widely used for classification, pattern recognition, and vector quantization. Typically, SOM networks have two layers of nodes: the input layer and the Kohonen layer, as shown in Fig. 1. The input layer is fully connected to the Kohonen layer, which is of two dimensions. During the training process, input data are fed to the network through the nodes in the input layer. As the training process proceeds, the nodes adjust their weight values according to the topological relations in the input data and also the neighborhood relations in the Kohonen layer. The node with the minimum distance is called the *winner* and adjusts its weights to be closer to the value of the input pattern.

Euclidian distance is the most common way of measuring the distance between vectors. Nevertheless, in this study, we adopt a *cost function* point of view that is similar to the energy function defined by Tatem [28] to be minimized in a Hopfield network to perform superresolution. This cost function will be defined in greater detail in Section III-B. It allows the twofold representation of the input layer to be taken into consideration. Input patterns integrate the coarse SPOT VEGETATION observation but also external knowledge such as the previous SPOT HRVIR spectral signatures in order to perform the fusion process.

Usually, the result of the training is that a pattern of organization emerges in the map. Different units learn to respond to different vectors in the input set, and units closer together will tend to respond to input vectors that are similar to each other. In this application, the organization that will result from the training will be the estimation of the spectral unmixing (i.e., the weight of the nodes) associated with the spatial location (i.e., the location of the nodes on the Kohonen layer) of the endmembers

to link the SPOT VEGETATION and the SPOT HRVIR resolutions. The size of the Kohonen layer has been fixed to 50×50 to fit the difference in resolution between the VEGETATION and HRVIR sensors.

During the iterative training, each neuron to be modified (the so-called winning neuron) of position (i_0, j_0) has its weight $w_t(i_0, j_0)$ modified in order to minimize the cost function as follows:

$$w_{t+1}(i, j) = w_t(i, j) - \alpha(t)\beta_t(i_0 - i, j_0 - j) \frac{\partial E}{\partial w(i_0, j_0)}$$

where $\alpha(t)$ modifies the weighting of the neurons and ensures convergence over iterations t ; and $\beta_t(\cdot)$ modifies the weighting of the neighborhood \mathcal{B}_0 of the winning neuron of position (i_0, j_0) .

$\alpha(t)$ takes its expression as

$$\alpha(t) = \begin{cases} \frac{1-e^{-(1+t)}}{1+t}, & \text{if } 0 \leq t \leq t_0 = T \left(1 - \frac{1}{\sqrt{\mathcal{B}_0}}\right) \\ \frac{1}{t-t_0}, & \text{if } t_0 < t < T. \end{cases}$$

Here, $e^{-(1+t)}$ avoids losing the local minima location at the beginning of the training, since it retains $\alpha(t)$ of limited value. In addition, convergence of the map is ensured, since $\sum_t \alpha(t) \rightarrow_{t \rightarrow +\infty} \infty$, while $\lim_{t \rightarrow +\infty} \sum_t \alpha(t)^2 \in \mathbb{R}$.

$\beta_t(\cdot)$ is dedicated to the neighborhood influence with

$$\beta_t(i_0 - i, j_0 - j) = \begin{cases} \frac{1}{1+(i-i_0)^2+(j-j_0)^2}, & \text{if } (i, j) \in \mathcal{B}_t(i_0, j_0) \\ 0, & \text{if not.} \end{cases}$$

Furthermore, the neighborhood itself is defined over iterations through

$$\mathcal{B}_t(i_0, j_0) = \mathcal{B}_0(i_0, j_0) \left(1 - \frac{t}{T}\right)^2.$$

B. Cost Function to be Minimized

The function E to minimize is defined in order to ensure the following conditions.

- 1) To respect the mixture. The mean of the overall map (the mean \hat{w} of the neurons $w(i, j)$, $1 \leq i, j \leq 50$) has to be as close as possible to the value of the collocated SPOT VEGETATION observation spectral signature \mathcal{V} , since a linear mixture is assumed. E_1 to be minimized is then defined as

$$E_1 = (\hat{w} - \mathcal{V})^2$$

$$\frac{\partial E_1}{\partial w(i_0, j_0)} = \frac{2}{z \times z} (\hat{w} - \mathcal{V}) \sum_{i,j} \beta(i_0 - i, j_0 - j).$$

- 2) To use external information such as
 - a) external map \mathcal{C} to define field boundaries;
 - b) field label for each pixel at the resolution of SPOT HRVIR: $n = \mathcal{C}(i, j)$;
 - c) centroid of each field label $\hat{w}|_n$ for field n .

From a thematic point of view, it is more convenient to characterize each field with its dominant spectral signature. This dominant spectral signature $\hat{w}|_n$ may come from long-term observations or from a simple classification of an older SPOT HRVIR observation (several scenarios will be shown in Section IV).

That is why the winning neuron of position (i_0, j_0) that belongs to the class or field number $n_0 = \mathcal{C}(i_0, j_0)$ is modified in order to be as close as possible to the dominant spectral signature $\hat{w}|_{n_0}$ of its class

$$E_2 = \frac{1}{\text{card}(n_0)} \sum_{\substack{i,j \\ \mathcal{C}(i,j)=n_0}} (w(i, j) - \hat{w}|_{n_0})^2.$$

$$\frac{\partial E_2}{\partial w(i_0, j_0)} = \frac{2}{\text{card}(n_0)} \left(\sum_{\substack{i,j \\ \mathcal{C}(i,j)=n_0}} \beta(i_0 - i, j_0 - j) w(i, j) - \hat{w}|_{n_0} \sum_{\substack{i,j \\ \mathcal{C}(i,j)=n_0}} \beta(i_0 - i, j_0 - j) \right).$$

This constraint tends to make fields homogeneous, and the knowledge of $\hat{w}|_n$ helps the initialization of the Kohonen map.

- 3) To use a "Change Potential" δ . In the case where the class \mathcal{C} represents roads or buildings, there is no change to be expected in our application. Nevertheless, when \mathcal{C} represents "bare soil" or "vegetation," some changes are to be expected. A precise analysis may be achieved field by field in order to give a parameter between 0 and 1 that gives the probability of the field being covered during the winter. More precisely, this change potential δ is defined for each field in $\{-1\} \cup [0, 1]$ as follows:

$$\begin{cases} \delta = 1, & \text{to force the estimation to a vegetation field;} \\ \frac{1}{2} < \delta < 1, & \text{to tend to a vegetation field;} \\ \delta = 1/2, & \text{do not interfere in the estimation;} \\ 0 < \delta < 1/2, & \text{to tend to a bare soil;} \\ \delta = 0, & \text{to force the estimation to a bare soil;} \\ \delta = -1, & \text{stop any change.} \end{cases}$$

This constraint modifies spectral signatures $w(i, j)$ toward a spectral signature \mathcal{S}_n that comes from a bare soil $\mathcal{S}_{\text{bare soil}}$ or a covered field $\mathcal{S}_{\text{covered}}$. Between these two bounds that correspond to $\delta = 0$ and $\delta = 1$, a spectral signature \mathcal{S}_n has to be defined with respect to δ

$$\mathcal{S}_n = \begin{cases} 2\delta w(i_0, j_0) + (1 - 2\delta)\mathcal{S}_{\text{bare soil}}, & \text{if } 0 \leq \delta \leq 1/2 \\ (2\delta - 1)\mathcal{S}_{\text{covered}} + 2(1 - \delta)w(i_0, j_0), & \text{if } 1/2 \leq \delta \leq 1 \\ w(i_0, j_0), & \text{if } \delta = -1 \end{cases}$$

when $\delta = -1$, $w(i_0, j_0)$ is not modified. When $\delta \neq -1$, the cost function E_3 is defined as

$$E_3 = \frac{1 - f(\delta)}{\text{card}(n_0)} \sum_{\substack{i,j \\ \mathcal{C}(i,j)=n_0}} (w(i, j) - \mathcal{S}_n)^2$$

$$\frac{\partial E_3}{\partial w(i_0, j_0)} = \frac{2(1 - f(\delta))}{\text{card}(n_0)} \left(\sum_{\substack{i,j \\ \mathcal{C}(i,j)=n_0}} \beta(i_0 - i, j_0 - j) w(i, j) - \mathcal{S}_n \sum_{\substack{i,j \\ \mathcal{C}(i,j)=n_0}} \beta(i_0 - i, j_0 - j) \right)$$

where $f(\delta)$ is a contrast function that does nothing when $\delta = (1/2)$ [e.g., $f(\delta) = (\sin(\pi\delta))^8$].



Fig. 2. Location of the study area. Aerial true color photograph draped on a 50-m resolution digital elevation model (source BD Ortho and DB Alti © IGN) with oblique view (inclination 45°, azimuth 180°, distance from center 5600 m). Red contour: watershed limits. (Upper right corner) IRS-WiFS December 8, 2001 showing Brittany, west of France. RGB composite (NIR, NIR, R).

When $\delta = (1/2)$, there is no change potential to be considered, and constraint E_3 becomes similar to E_2 . When using a change potential, E_2 is modified in the same way by considering $f(\delta)E_2$ instead.

Spectral signatures $S_{\text{bare soil}}$ and S_{covered} are evaluated with older observations of SPOT HRVIR and a selection of the spectral signatures to be considered through their NDVI values. In fact, the *normalized difference vegetation index*, defined by $(\text{NIR} - R)/(\text{NIR} + R)$ is an appropriate tool to select the most representative spectral signatures to define $S_{\text{bare soil}}$ as bare field and S_{covered} as field covered with vegetation.

The training process produces a map where the patterns are organized in order to minimize $E = E_1 + f(\delta)E_2 + E_3(\delta)$ so that the weight vector of the neurons corresponds to the estimation of the mixture of the SPOT VEGETATION observation at the scale of the SPOT HRVIR with their location.

It is understood that only three bands out of the four of VEGETATION and HRVIR may be considered, i.e., 0.61–0.68, 0.78–0.89, and 1.58–1.75 μm , since the bands B0 and B1 are not sensitive to the same wavelength (see Table I).

IV. EXPERIMENTS

The methodology was applied to the *Coët-Dan* watershed, a 1210-ha area, located in Central Brittany, which is characterized by a fragmented landscape mosaic of small fields surrounded partly by hedges (Fig. 2). This study area is considered as representative of the intensive agricultural watersheds of the region, where the water quality is degraded, mainly due to nonpoint source pollution. The *Coët-Dan* watershed has been instrumented since 1973 for evaluating and characterizing hydrologic processes, land cover, and land use associated with farming practices [29].

A series of images from SPOT VEGETATION and SPOT HRVIR sensors was acquired for a three-year period, from 1999 to 2001. Images (from P products) were corrected for geometric

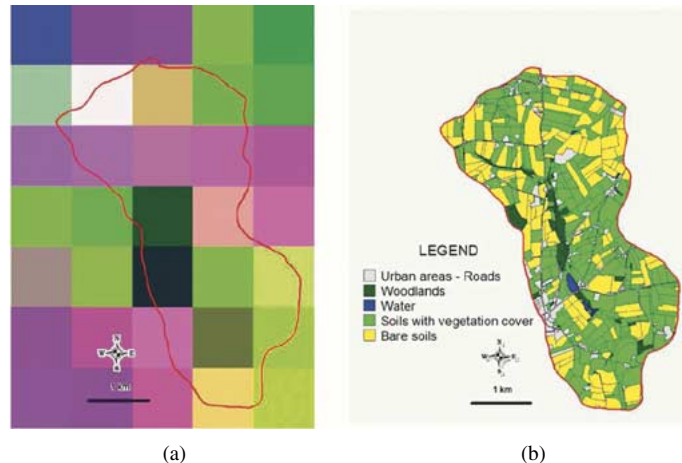


Fig. 3. *A priori* knowledge (a) SPOT VEGETATION observation for winter 2000–2001 (12/17/2001) and (b) ground use for each field for winter 2000–2001. (a) SPOT VEGETATION December 17, 2001 and the contour of the study area RGB false-color composite (MIR, NIR, R). (b) Ground use map of the study area winter land cover 2002 (December 3, 2001).

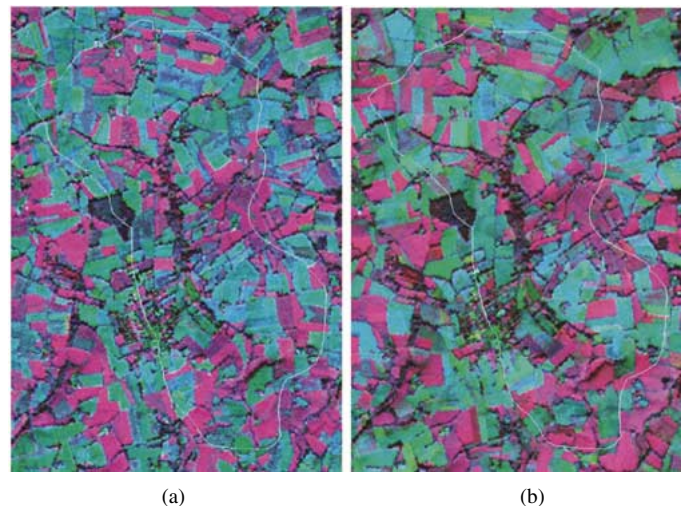


Fig. 4. Result of mixture estimation and spatial location by the Kohonen map and comparison with true SPOT HRVIR observation. (a) HRVIR estimation for winter 2000–2001. (b) True SPOT HRVIR observation for winter 2000–2001. RGB false color composites (MIR, NIR, R).

distortions and were calibrated to reflectance by using the 5S model [30]. In this case, the ratio bare soil/vegetation was estimated at local scale for the winter 2000–2001.

As shown in Fig. 3, a 5×7 block of the SPOT VEGETATION observation fits the watershed. Each field of the watershed is structurally defined by external knowledge map \mathcal{C} and labeled. In fact, field map \mathcal{C} was carried out both from the SPOT HRVIR image of the previous winter and from expert knowledge.

Mixture estimation and location results are shown in Fig. 4. This estimation corresponds to the local land cover for the winter 2000–2001 at a resolution of 20 m, taking into consideration the SPOT VEGETATION 1-km observation and the change potential of each field. Comparisons with true SPOT HRVIR observations acquired during the winter 2000–2001 proved that the estimation of the mixture by a Kohonen map and the location of endmembers is relevant. A finer analysis shows that the spectral signatures yielded by each neuron are similar to the observed data.

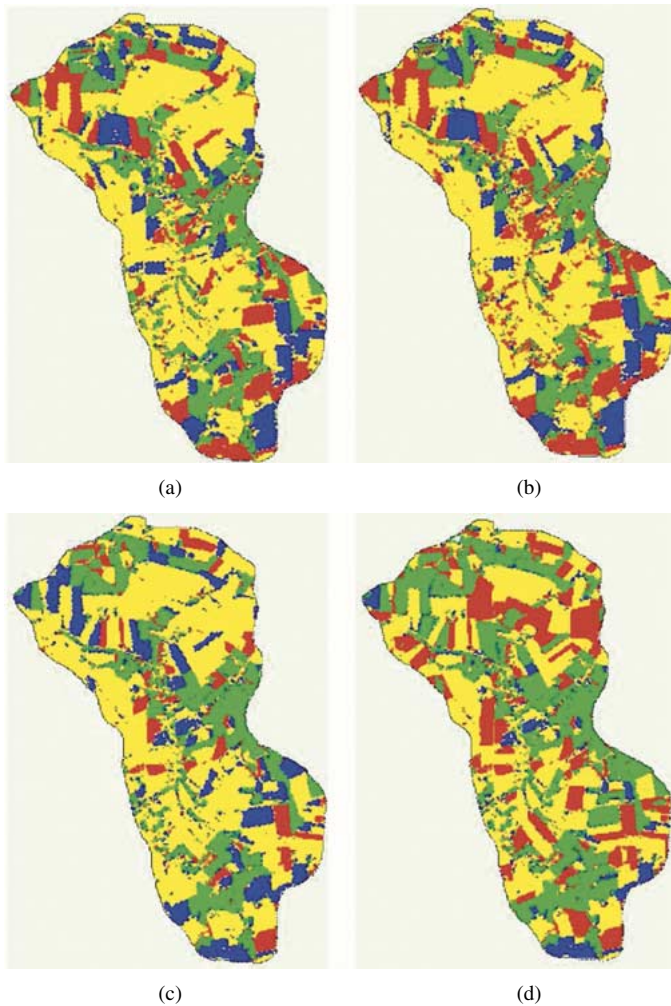


Fig. 5. Estimation of the “Bare soils” and “Soils with vegetation cover” from the mixture acquired by SPOT VEGETATION for the winter 2000–2001. Four scenarios are defined to obtain field boundary and land-cover knowledge. (a) NDVI estimation for each spectral signature ($E_1 + E_2$). (b) Field structure as external knowledge and classification of land cover. (c) Potential change map with the pessimistic hypothesis “fields will not be covered.” (d) Potential change map with the optimistic hypothesis “fields will be covered.” (Yellow) Bare soils (well estimated). (Green) Soils with vegetation (well estimated). (Red) Bare soils (bad estimated). (Blue) Soils with vegetation (bad estimated).

In fact, different scenarios were assessed for the estimation of fields’ spectral signatures $\hat{w}|_n$. The first two scenarios do not take into consideration potential change δ .

- The first scenario does not require external information, but previous SPOT HRVIR observations. Only the cost function $E = E_1 + E_2$ is considered for training the Kohonen maps. From this previous observation acquired in the winter 1999–2000, an NDVI was estimated for each pixel (at 20 m of resolution) and classified as “Bare soils” or “Soils with vegetation.” Two spectral signatures were evaluated for $\hat{w}|_{\text{Bare soils}}$ and $\hat{w}|_{\text{Soils with vegetation}}$. This classification also yielded an estimation of the map \mathcal{C} as a set of fields with similar coverage rate. As shown in Fig. 5(a) and Table II(a), accuracy of the estimation of “Bare soils” or “Soils with vegetation” is 67.5%.
- The second scenario takes into consideration ground observations in order to use the field map \mathcal{C} as external knowledge, while the Kohonen map is still trained with

TABLE II
NUMERICAL RESULTS FROM THE DIFFERENT SCENARIOS FOR ESTIMATING “BARE SOILS” AND “SOILS WITH VEGETATION COVER” FROM THE MIXTURE ACQUIRED BY SPOT VEGETATION FOR THE WINTER 2000–2001 (SEE ALSO FIG. 5)

Scenarios		Bare soils	Soils with vegetation	Total	Overall accuracy
(a)	Bare Soils	571.4	220.8	792.2	67.5 %
	Soils with vegetation	172.5	245.5	418.0	
	Total	743.9	466.3	1210.2	
(b)	Bare Soils	580.5	252.9	833.4	65.7 %
	Soils with vegetation	162.7	214.1	376.8	
	Total	743.2	467.0	1210.2	
(c)	Bare Soils	622.8	120.3	743.1	72.9 %
	Soils with vegetation	208.4	258.7	467.1	
	Total	831.2	379.0	1210.2	
(d)	Bare Soils	473.8	269.3	743.1	69.3 %
	Soils with vegetation	102.0	365.1	467.1	
	Total	575.8	634.4	1210.2	

surface in ha.

the cost function $E_1 + E_2$ with no change potential. An NDVI was evaluated for each field and then affected to a “bare soil” or “soil with vegetation” class. Despite the finer land use classification, the estimation accuracy is not better [65.7% as shown in Fig. 5(b) and Table II(b)].

A rejected class had been considered for these two cases when the NDVI did not sound with chlorophyllian cover (such as buildings, roads, or water from lakes, etc.).

Other scenarios were defined by considering temporal behavior through a potential change map defined for each field for the winter 2000–2001. The potential change was evaluated by considering the dynamics in crop rotations over the previous six years and classified according to the kind of agricultural practices. Moreover, two hypothesis were considered in order to integrate policy incentives or advice. In fact, farmers’ behavior is integrated with a pessimistic or optimistic hypothesis as follows.

- The first hypothesis considers that farmers would not follow advice and would rather leave their fields according to standard crop rotations.
- The other took the hypothesis that they would apply better agricultural practices by covering their fields during the winter. Hence, standard crop rotation is becoming modified by policy incentives.

For these two scenarios, HRVIR estimation for the winter 2000–2001 was achieved with the cost function $E_1 + f(\delta)E_2 + E_3(\delta)$. By including the potential change map, the estimation accuracy is better and rises to 72.9%. The estimation accuracy is better in the first case [scenario (c)], which means that in fact, farmers did not follow the advice and mainly left their fields without vegetation, on average, in the same proportion as during the previous winters.

V. CONCLUSION

The study presented is dedicated to characterizing land-cover changes, detected at a coarse scale, with high-resolution considerations. The use of the Kohonen map that takes into con-

sideration *a priori* knowledge by integrating potential temporal change for training proved to be an interesting alternative for processing images having different resolutions. However, the high-difference in spatial resolution between the two sensors used—SPOT VEGETATION and SPOT HRVIR—limits the location accuracy of the land-cover classes.

At this stage, in such a fragmented landscape, the estimation accuracy of the bare soil/vegetation ratio is strongly limited by the coarse spatial resolution of the SPOT VEGETATION sensor. Several experiments could be performed with images that are potentially more adapted to land-cover monitoring in fragmented landscapes, since medium spatial resolution sensors with a daily repetition rate are now available. Thus, the use of images from the Earth Observing System Moderate Resolution Imaging Spectroradiometer Terra or ENVISAT Medium Resolution Imaging Spectrometer with colocated high-resolution observations such as SPOT HRVIR should improve the estimation of the bare soil/vegetation ratio during the fallow and planting seasons.

ACKNOWLEDGMENT

The authors would like to thank P. Bordenave and T. Bioteau (CEMAGREF Rennes) for providing ground observations on the study area.

REFERENCES

[1] S.-M. Dabney, J.-A. Delgado, and D.-W. Reeves, "Using winter cover crops to improve soil and water quality," *Commun. Soil Sci. Plant Anal.*, vol. 32, no. 7 & 8, pp. 1221–1250, 2001.

[2] T. Houet, L. Hubert-Moy, and G. Mercier. (2004) Modélisation du changement d'échelles en télédétection par une méthode neuronale; application à l'étude de l'évolution de l'occupation hivernale des sols en Bretagne. [Online]. Available: <http://193.55.107.45/eurogeo2.htm>.

[3] J. Sveinsson and J. Benediktsson, "Data fusion and feature extraction using tree structured filter banks," in *Proc. IGARSS*, vol. 6, Jul. 24–28, 2000, pp. 2617–2619.

[4] B. Aiazzi, L. Alparone, F. Argenti, S. Baronti, and I. Pippi, "Multisensor image fusion by frequency spectrum substitution: Subband and multirate approaches for a 3:5 scale ratio case," in *Proc. IGARSS*, vol. 6, Jul. 24–28, 2000, pp. 2629–2631.

[5] D. Tseng, Y. Chen, and M. Liu, "Wavelet-based multispectral image fusion," in *Proc. IGARSS*, vol. 4, Jul. 9–13, 2001, pp. 1956–1958.

[6] B. Aiazzi, L. Alparone, A. Barducci, S. Baronti, and I. Pippi, "Multispectral fusion of multisensor image data by the generalized laplacian pyramid," in *Proc. IGARSS*, vol. 2, 1999, pp. 1183–1185.

[7] B. Escalante-Ramirez and A. Lopez-Caloca, "Image fusion with the Hermite transform," in *Proc. Int. Conf. Image Processing*, vol. 2, Sep. 14–17, 2003, pp. 145–148.

[8] M. Basseville, A. Benveniste, K. Chou, S. Golden, R. Nikoukhah, and A. Willsky, "Modeling and estimation of multiresolution stochastic process," *IEEE Trans. Inform. Theory*, vol. 38, no. 2, pp. 766–784, Mar. 1992.

[9] L. Wald and T. Ranchin, "The ARSIS concept in image fusion: An answer to users needs," in *Proc. 6th Int. Conf. Information Fusion*, vol. 1, Jul. 8–11, 2003, pp. 168–173.

[10] H. Krim, A. Willsky, and W. Karl, "Multiresolution models for random fields and their use in statistical image processing," in *IEEE-IMS Workshop on Information Theory and Statistics*, Oct. 27–29, 1994, p. 56.

[11] A. Winter, H. Maître, N. Cambou, and E. Legrand, "An original multisensor approach to scale-based image analysis for aerial and satellite images," in *Proc. Int. Conf. Image Processing*, vol. 2, Oct. 1997, pp. 234–237.

[12] S. L. Hegarat-Masclé, D. Richard, and C. Otle, "Multi-scale data fusion using Dempster-Shafer evidence theory," in *Proc. IGARSS*, vol. 2, Jun. 24–28, 2002, pp. 911–913.

[13] G. Cliche, F. Bonn, and P. Teillet, "Integration of the panchromatic channel into its multispectral mode for image sharpness enhancement," *Photogramm. Eng. Remote Sens.*, vol. 51, no. 3, pp. 311–316, Mar. 1985.

[14] W.-J. Carper, T.-M. Lillesand, and R.-W. Kiefer, "The use of intensity-hue-saturation transformations for merging SPOT panchromatic and multispectral image data," *Photogramm. Eng. Remote Sens.*, vol. 56, no. 4, pp. 459–467, Apr. 1990.

[15] P.-S. Chavez, S.-C. Sides, and A. Anderson, "Comparison of three different methods to merge multiresolution and multispectral data: Landsat TM and SPOT panchromatic," *Photogramm. Eng. Remote Sens.*, vol. 57, pp. 295–303, 1991.

[16] X. Liu, F. Xiong, and W. Sun, "Interpolation of HIRS/2 images using AVHRR image and its application," in *Proc. IGARSS*, vol. 3, 1993, pp. 1487–1489.

[17] A. Minghelli-Roman, M. Mangolini, M. Petit, and L. Polidori, "Spatial resolution improvement of MeRIS images by fusion with TM images," *IEEE Trans. Geosci. Remote Sensing*, vol. 39, no. 7, pp. 1533–1536, Jul. 2001.

[18] Z. Jiao, X. Li, J. Wang, and G. Yan, "Classification-based fusion of IKONOS 1-m high-resolution panchromatic image and 4-m multi-spectral images," in *Proc. IGARSS*, vol. 2, Jul. 9–13, 2001, pp. 703–705.

[19] V. Petrović and C. Xydeas, "Gradient-based multiresolution image fusion," *IEEE Trans. Image Process.*, vol. 13, no. 2, pp. 228–237, Feb. 2004.

[20] S. Bouzidi, J. Berroir, and I. Herlin, "A remote sensing data fusion approach to monitor agricultural areas," in *Proc. 14th Int. Conf. Pattern Recognition*, vol. 2, Aug. 16–20, 1998, pp. 1387–1389.

[21] J. Susaki and R. Shibasaki, "Fusion of AVHRR and TM data for vegetation classification based on unmixing technique," in *Proc. IGARSS*, vol. 6, Jul. 24–28, 2000, pp. 2423–2425.

[22] H. Cardot, R. Faivre, and M. Goulard, "Functional approaches for predicting land use with the temporal evolution of coarse resolution remote sensing data," *J. Appl. Stat.*, vol. 29, pp. 1195–1199, 2003.

[23] G. Carpenter, S. Gopal, S. Macomber, S. Martens, and C. Woodcock, "A neural network method for mixture estimation for vegetation mapping," *Remote Sens. Environ.*, vol. 70, no. 2, pp. 138–152, 1999.

[24] S. Baglio, S. Graziani, G. Manganaro, and N. Pitrone, "Cellular neural networks: A new paradigm for multisensor data fusion," in *Proc. 8th Mediterranean Electrotechnical Conf.*, vol. 1, May 13–16, 1996, pp. 50–512.

[25] F. Melgani, S. Serpico, and G. Vernazza, "Fusion of multitemporal contextual information by neural networks for multisensor image classification," in *Proc. IGARSS*, vol. 7, Jul. 9–13, 2001, pp. 2952–2954.

[26] A. Tatem, H. Lewis, P. Atkinson, and M. Nixon, "Super-resolution target identification from remotely-sensed images using a Hopfield neural network," *IEEE Trans. Geosci. Remote Sens.*, vol. 39, no. 4, pp. 781–796, Apr. 2001.

[27] T. Kohonen, "The self-organizing map," *Proc. IEEE*, vol. 78, no. 9, pp. 1464–1480, Sep. 1990.

[28] A. Tatem, H. Lewis, P. M. Atkinson, and M. S. Nixon, "Super-resolution mapping of urban scenes from IKONOS imagery using a Hopfield neural network," in *Proc. IGARSS*, vol. 7, 2001, pp. 3203–3205.

[29] L. Hubert-Moy, "Analyse de la structure spatiale de l'occupation des sols par télédétection," in *Agriculture Intensive et Qualité des Eaux*, C. Cheverry, Ed. Paris, France: INRA, 1998, pp. 41–52.

[30] D. Tanré, C. Deroo, P. Duhaut, M. Herman, J. Moquette, J. Perbos, and P. Deschamps, "Description of a computer code to simulate the satellite signal in the solar spectrum: The 5 S code," *Int. J. Remote Sens.*, vol. 11, no. 4, pp. 559–668, 1990.



Grégoire Mercier (M'01) graduated from the Institut National des Télécommunications (INT), Evry, France, in 1993, and received the Ph.D. degree from the University of Rennes I, Rennes, France, in 1999.

He is currently an Associate Professor at the Ecole Nationale Supérieure des Télécommunications de Bretagne (ENST Bretagne), Brest, France, where his current research is on remotely sensed image processing, focused on the compression and the segmentation of SAR and hyperspectral data. His work is mostly dedicated to change detection for risk

management and oil slick detection from SAR and hyperspectral images.



Laurence Hubert-Moy received the Ph.D. degree in geography from the University of Rennes II, Rennes, France.

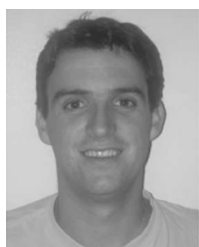
Since 1989, she has been an Associate Professor with the Department of Geography, University of Rennes II. She was with the Department of Geography, Center for Remote Sensing, Boston University, MA as a Visiting Scientist in 1997, and she served as a Research Scientist from 2000 to 2002 at CNRS (French National Center for Scientific Research). Her research has extensively focused in the area of agriculture applications of remote sensing data. Specifically, she focused her efforts in various critical areas such as the local and regional land cover and land-cover change mapping in intensive farming areas; wetlands identification and characterization with remote sensing data; and spatial modeling and spatial statistics as applied to image understanding and use.

Dr. Hubert-Moy received the Bronze Medal of the French National Center for Scientific Research in 2003.



Pascal Gouéry received the Diplôme d'Etudes Approfondies in computer science from the University of Rennes II, Rennes, France, in 1987.

He is currently a Computer Engineer with the University of Rennes II. Since 1998, he has worked with the Climat et Occupation du Sol par Télédétection (COSTEL), University of Rennes II as data processing expert.



Thomas Houet was born in Rennes, France, in 1978. He received the M.S. degree in geography from the University of Rennes II, Rennes, France, in 2001. He is currently pursuing the Ph.D. degree at the Climat et Occupation du Sol par Télédétection (COSTEL), University of Rennes.

Since 2001, he has specialized in GIS and remote sensing technologies applied to Planning and the Environment. His main research interests are in observing, understanding, and modeling land-use/land-cover and landscapes features changes at different scales. He is using cellular automaton methods with GIS and remotely sensed tools to provide a basis for projecting land-use changes in considering landscapes features and simulate plausible future states.